Supporting Information for

Dinuclear Ag(I) Metallamacrocycles of Bis-N-Heterocyclic Carbenes Bridged by Calixarene Fragments: Synthesis, Structure and Chemosensing Behavior

Cai-Xia Lin,[b] Xiao-Fei Kong,[a] Qing-Shan Li,[a] Zheng-Zhi Zhang,*[a] Yao-Feng Yuan *[b] and Feng-Bo Xu *[a]

Table of Contents

Table S1. C-H···F hydrogen-bonds in the crystal structures of complexes **6a~f**. (Å, °)

	H–bond	D–H	H···A	D···A	D–H···A	Symmetry codes
6a	C(1)-H(1B)···F(4)	0.98	2.41	3.315(3)	154	0.5 + x, -0.5 + y, 0.5 - z
	C(1)-H(1C)···F(2)	0.98	2.36	3.237(3)	148	1- x, -y, z
6b	C(2)-H(2)···F(4)	0.95	2.52	3.25(2)	133	0.5 - x, -0.5 + y, 0.5 - z
	C(7)-H(7)···F(10)	0.95	2.45	3.39(3)	170	x, y, -1 + z
	C(9)-H(9)···F(3)	0.95	2.55	3.480(19)	168	-
	C(19)-H(19)···F(9)	0.95	2.39	3.18(4)	140	0.5 – x, -0.5 + y, 1.5 - z
	C(22)-H(22B)···F(7)	0.98	2.37	3.23(2)	145	1 - x, -y, 1 - z
	C(22)-H(22C)···F(12)	0.98	2.39	3.09(2)	127	x, -1 + y, -1 + z
	C(36)-H(36A)···F(1)	0.98	2.49	3.44(2)	162	0.5 + x, 0.5 - y, -0.5 + z
	C(37)-H(37C)···F(8)	0.98	2.51	3.47(3)	165	0.5 + x, 0.5 - y, -0.5 + z
6c	C(23)-H(23C)···F(4)	0.98	2.27	3.119(4)	144	1- x, 1-y, 1- z
	C(40)-H(40A)···F(1)	0.98	2.28	3.173(6)	151	1- x, 1- y, -z
	C(28)-H(28A)···N(5)	0.99	2.62	3.475(10)	145	-x, 1- y, 1- z
	C(40)-H(40B)···O(1)	0.98	2.54	3.44(2)	133	-
6d	C(7)-H(7)···F(4)	0.95	2.50	3.398(9)	157	1 + x, y, z
	C(17)-H(17)···F(5)	0.95	2.55	3.320(11)	139	0.5 + x, 0.5 - y, -0.5 + z
	C(19)-H(19A)···F(6)	0.99	2.37	3.343(9)	168	0.5 + x, 0.5 - y, -0.5 + z
	C(29)-H(29)···N(6)	0.95	2.56	3.418(11)	150	1.5 - x, 0.5 - y, 1 - z
	C(40)-H(40)···F(1)	0.95	2.39	3.337(10)	174	1 - x, -y, 1 - z
6e	C(3) -H(3)···F(3)	0.95	2.48	3.353(9)	152	-
	C(11)-H(11)···F(6)	0.95	2.53	3.428(7)	157	1- x, -y, 1- z
	C(17)-H(17)···F(8)	0.95	2.55	3.292(6)	135	1- x, -y, 1- z
	C(27)-H(27B)···F(12)	0.98	2.24	3.076(18)	143	x, y, -1 + z
	C(28)-H(28A)···F(11)	0.99	2.27	3.234(14)	163	x, y, -1 + z
	C(36)-H(36A)···F(11)	0.98	2.54	3.492(12)	165	x, y, -1 + z
	C(39)-H(39)···N(10)	0.95	2.23	3.112(12)	155	1- x, -y, -z
	C(66)-H(66)···F(9)	0.95	2.53	3.408(6)	154	1 + x, y, -1 + z

Continued

	H–bond	D–H	H···A	D···A	D–H···A	Symmetry codes
	C(71)-H(71)···F(4)	0.95	2.53	3.450(6)	164	1- x, 1- y, -z
	C(81)-H(81C)···F(10)	0.98	2.52	3.452(15)	159	x, y, -1 + z
	C(82)-H(82C)···F(1)	0.98	2.51	3.457(8)	163	x, y, -1 + z
	C(94)-H(94)···F(1)	0.95	2.43	3.224(7)	140	1- x, 1- y, 1- z
	C(96)-H(96B)···F(1)	0.99	2.54	3.337(7)	138	1- x, 1- y, 1- z
	C(96)-H(96B)···F(4)	0.99	2.48	3.294(6)	139	1- x, 1- y, 1- z
	C(104)-H(104)···F(9)	0.95	2.35	3.286(8)	170	1 + x, y, z
	C(107)--H(107)···F(13)	0.95	1.99	2.87(2)	153	2 - x, 1 - y, 1 - z
	C(107)--H(107)···F(14)	0.95	2.26	2.946(16)	129	2 - x, 1 - y, 1 - z
6f	C(11)-H(11)···F(6)	0.95	2.44	3.383(6)	172	-
	C(15)-H(15A)···F(1)	0.99	2.36	3.327(5)	165	1 - x, 1 - y, 1 - z
	C(63)-H(63)···F(1)	0.95	2.55	3.393(4)	149	x, 1 + y, z
	C(70)-H(70)···F(4)	0.95	2.36	3.251(6)	156	2 - x, 1 - y, 1 - z

Table S2. Distances (Å) of intermolecular π-π interactions for complexes **6c~f.**

Compounds	interacted rings	Face-to-Face	Center-to-Center	Symmetry Code
6c	naphthalene	3.2915(13)	3.820(2)	1 - x, -y, 1 - z
6d	anthracene	3.367(3)	3.955(4)	2.5 - x, 0.5 - y, 1 - z
6e	anthracene	3.4124(16)	3.953(3)	2 - x,1 - y, -1 - z
6f	anthracene	3.3705(11)	3.6135(18)	2 - x, 2 - y, 1 - z

^{1}H NMR spectra of complexes 6a~f and ligands 5a~f

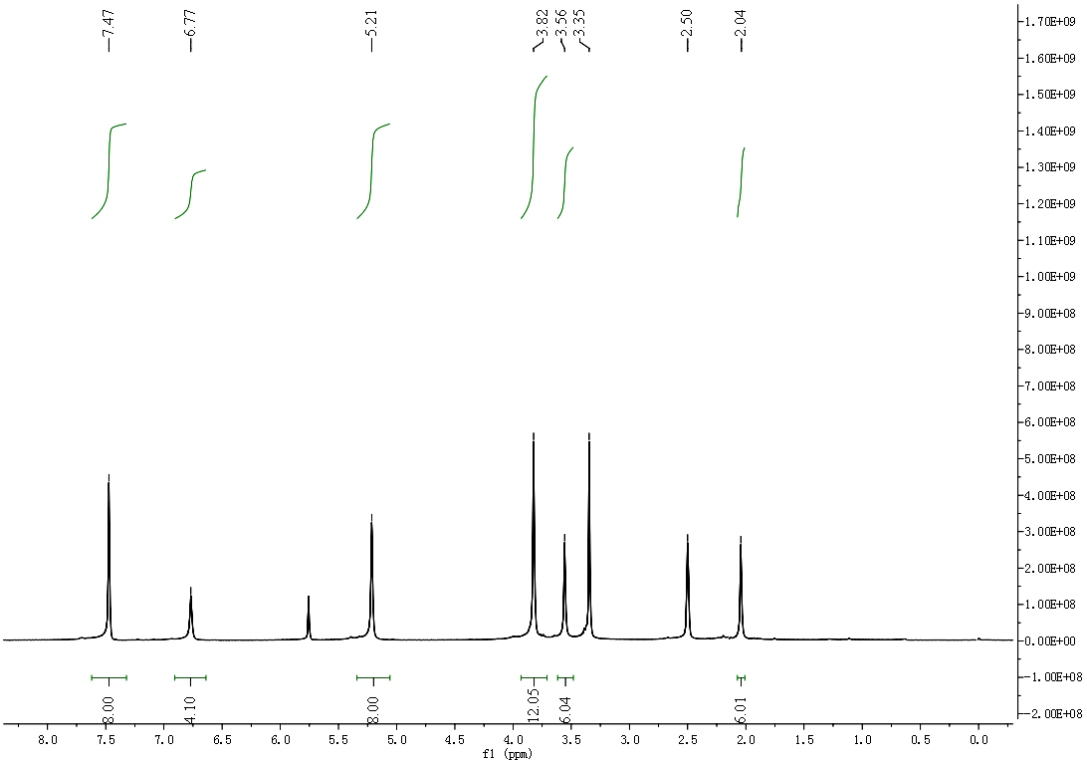

Figure S1. ^{1}H NMR spectrum for **6a** (400 MHz, DMSO-d_6, 298 K)**.**

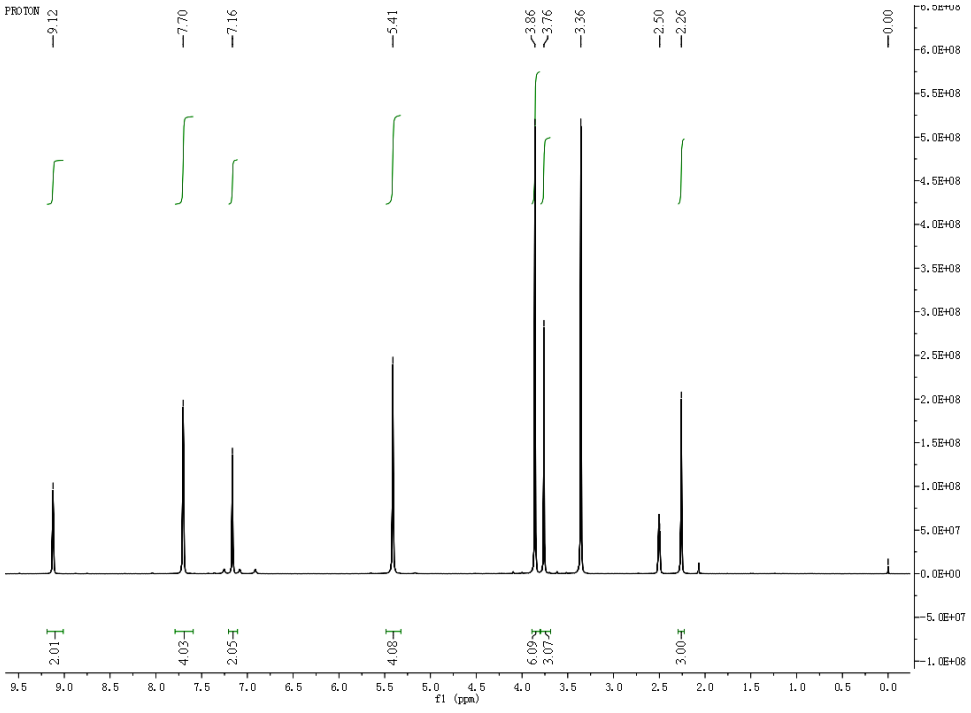

Figure S2. ^{1}H NMR spectrum for ligand **5a** (400 MHz, DMSO-d_6, 298 K)**.**

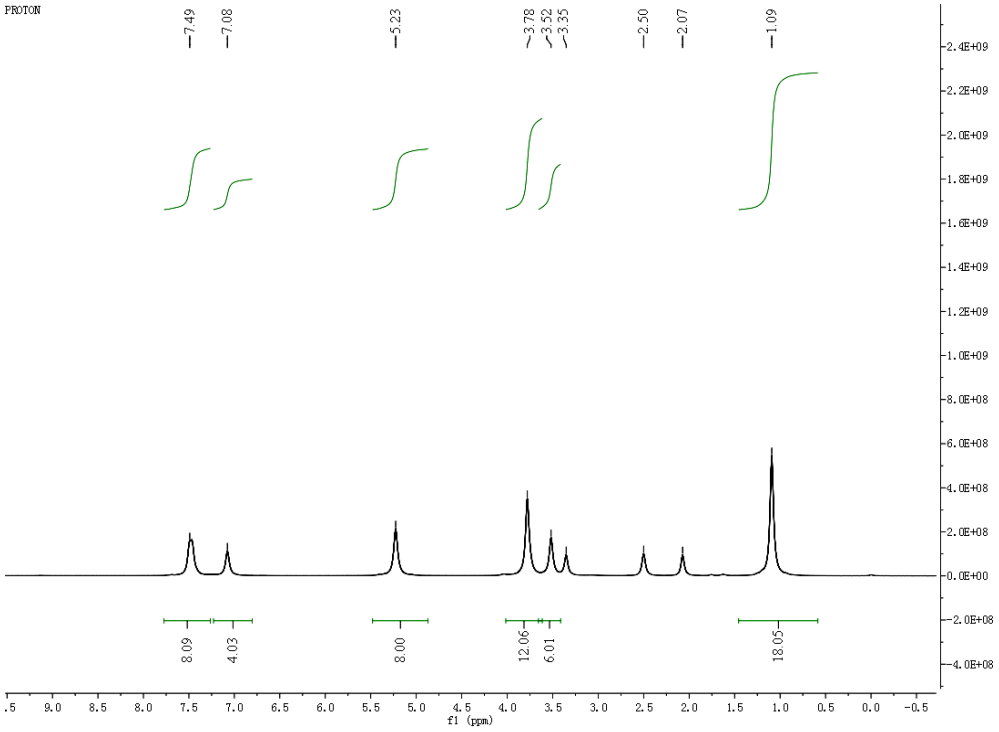

Figure S3. ^{1}H NMR spectrum for complex **6b** (400 MHz, DMSO-d_6, 298 K)**.**

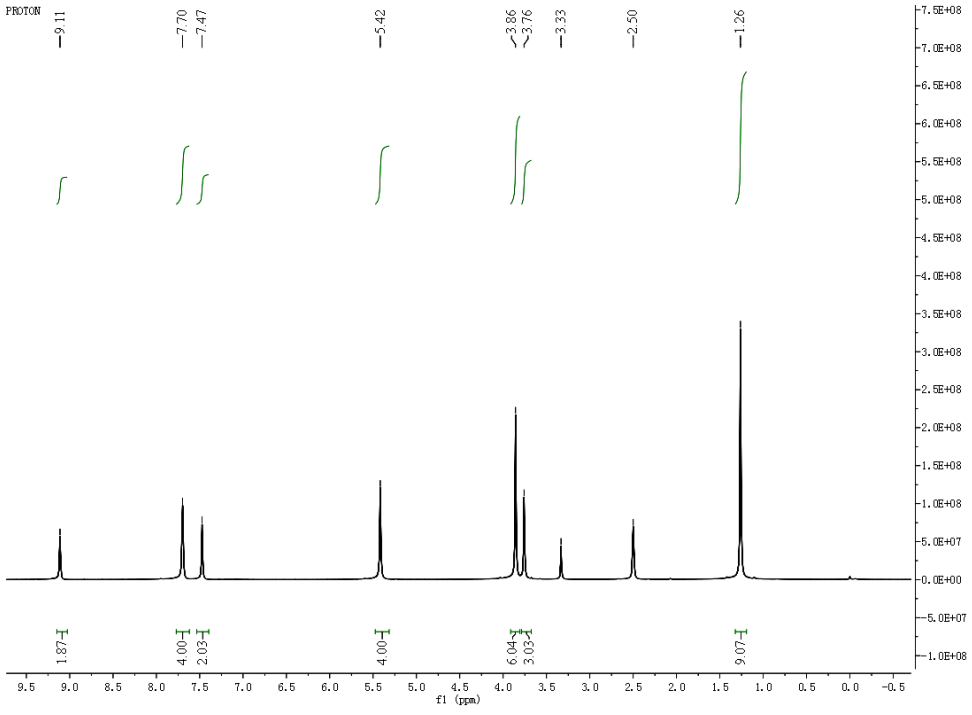

Figure S4. ^{1}H NMR spectrum for ligand **5b** (400 MHz, DMSO-d_6, 298 K)**.**

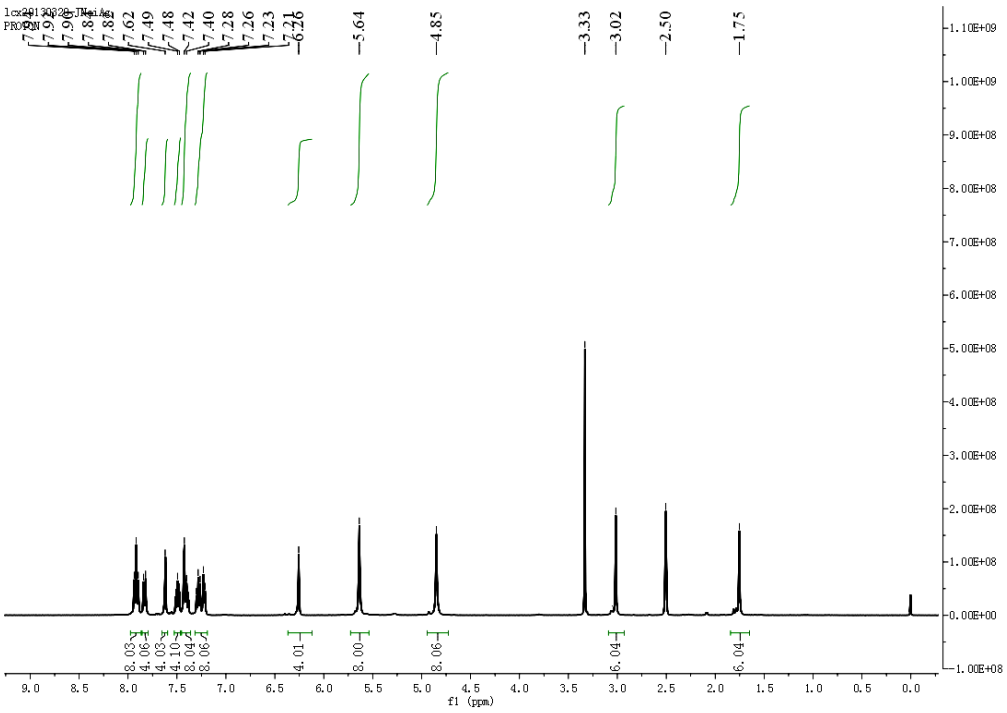

Figure S5. ^{1}H NMR spectrum for complex **6c** (400 MHz, DMSO-d_6, 298 K)**.**

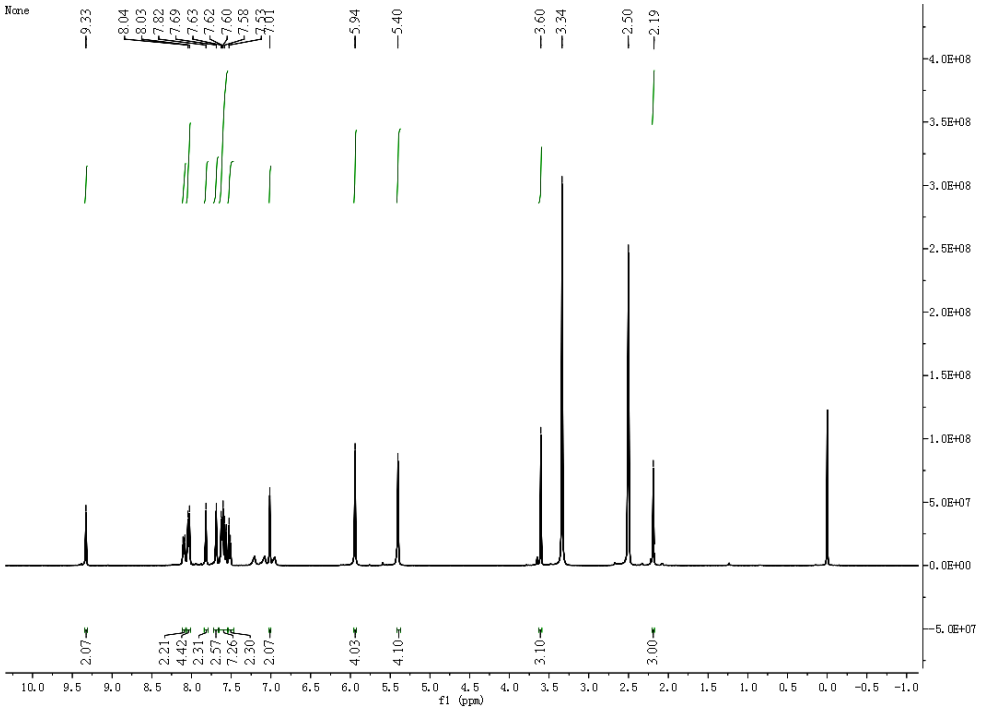

Figure S6. ^{1}H NMR spectrum for ligand **5c** (400 MHz, DMSO-d_6, 298 K)**.**

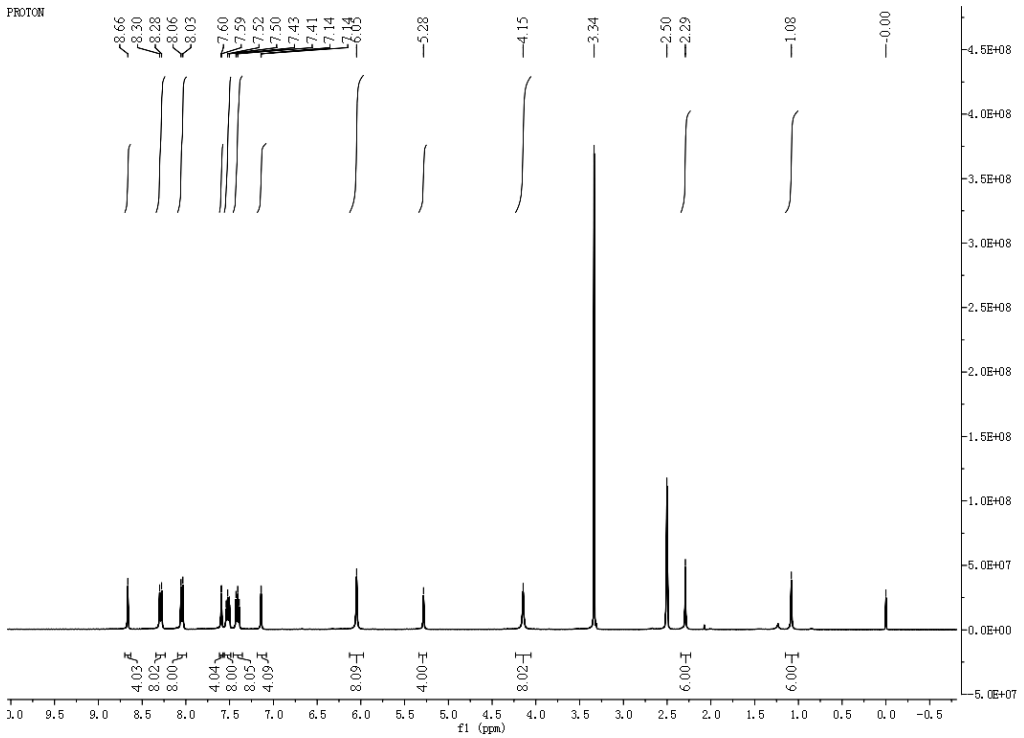

Figure S7. ^{1}H NMR spectrum for complex **6d** (400 MHz, DMSO-d_6, 298 K)**.**

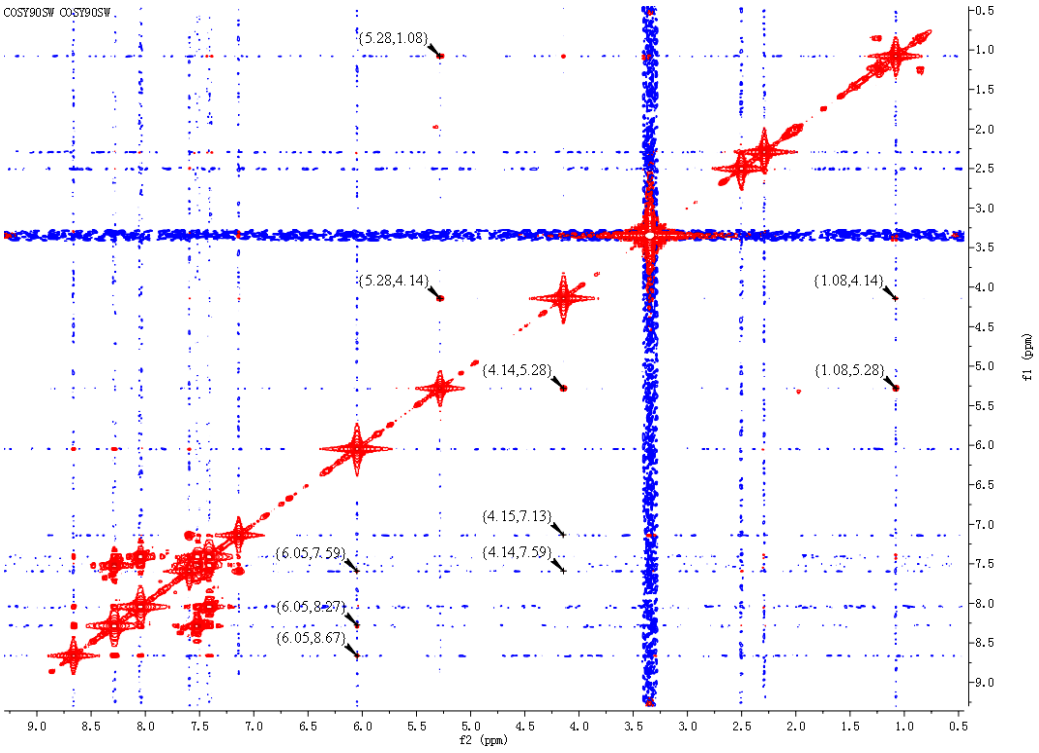

Figure S8. H-H COSY spectrum for complex **6d** (400 MHz, DMSO-d_6, 298 K)**.**

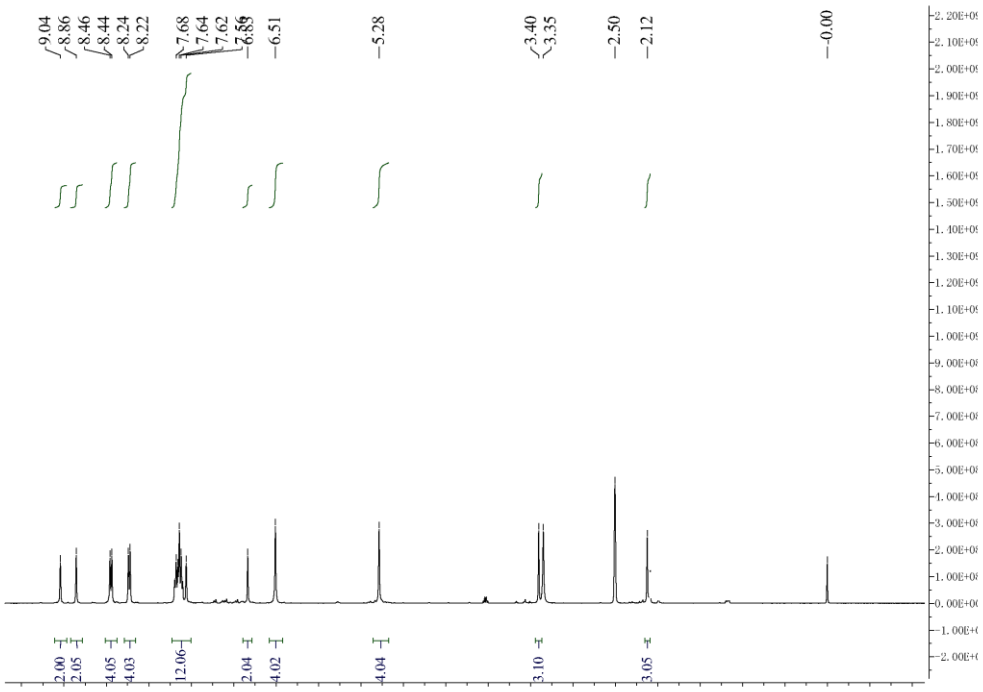

Figure S9. ^{1}H NMR spectrum for ligand **5d** (400 MHz, DMSO-d_6, 298 K)**.**

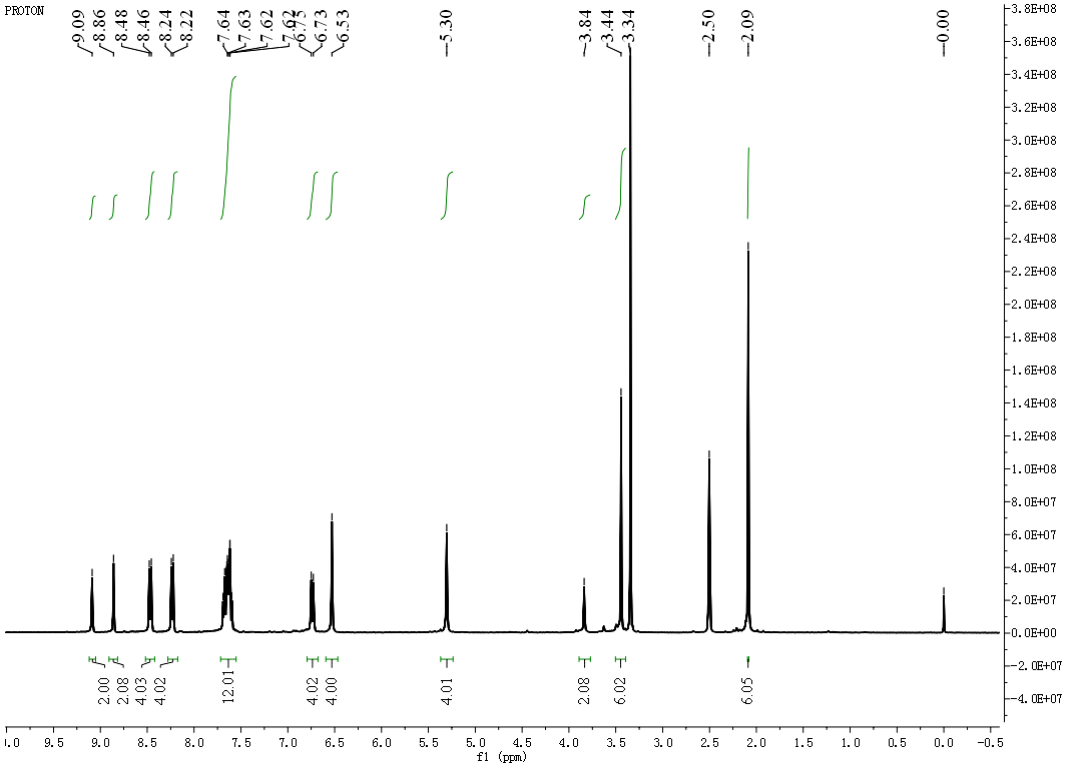

Figure S10. ^{1}H NMR spectrum for ligand **5e** (400 MHz, DMSO-d_6, 298 K).

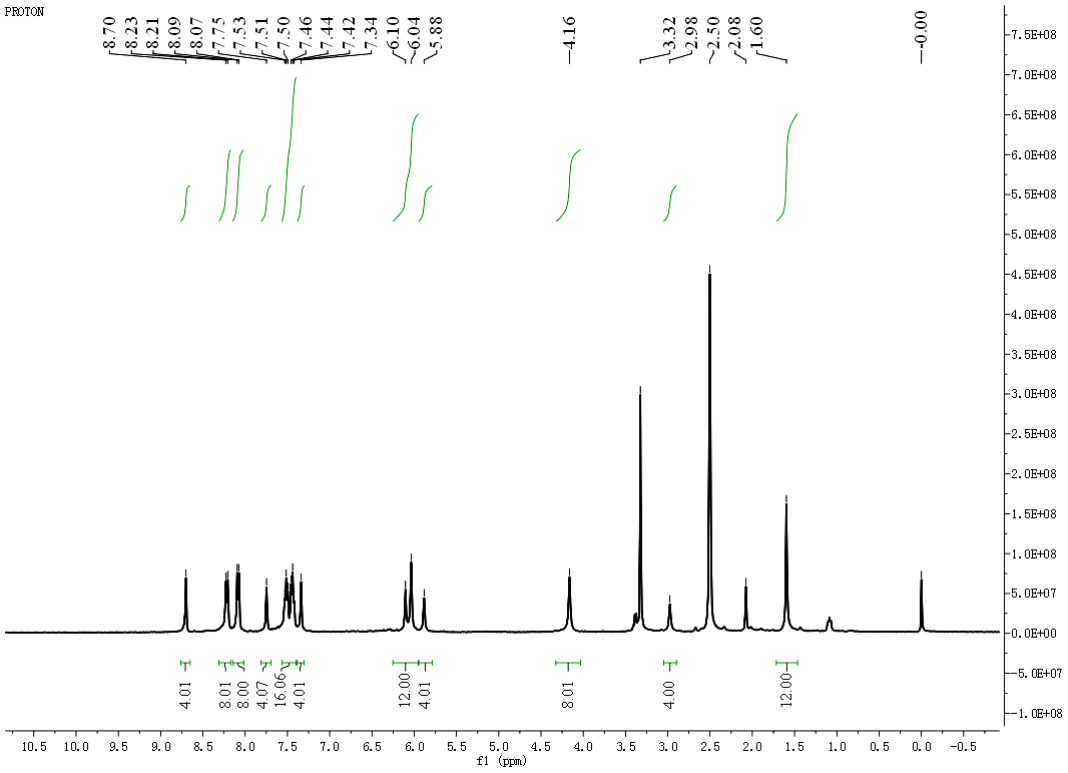

Figure S11. ^{1}H NMR spectrum for complex **6e** (400 MHz, DMSO-d_6, 298 K).

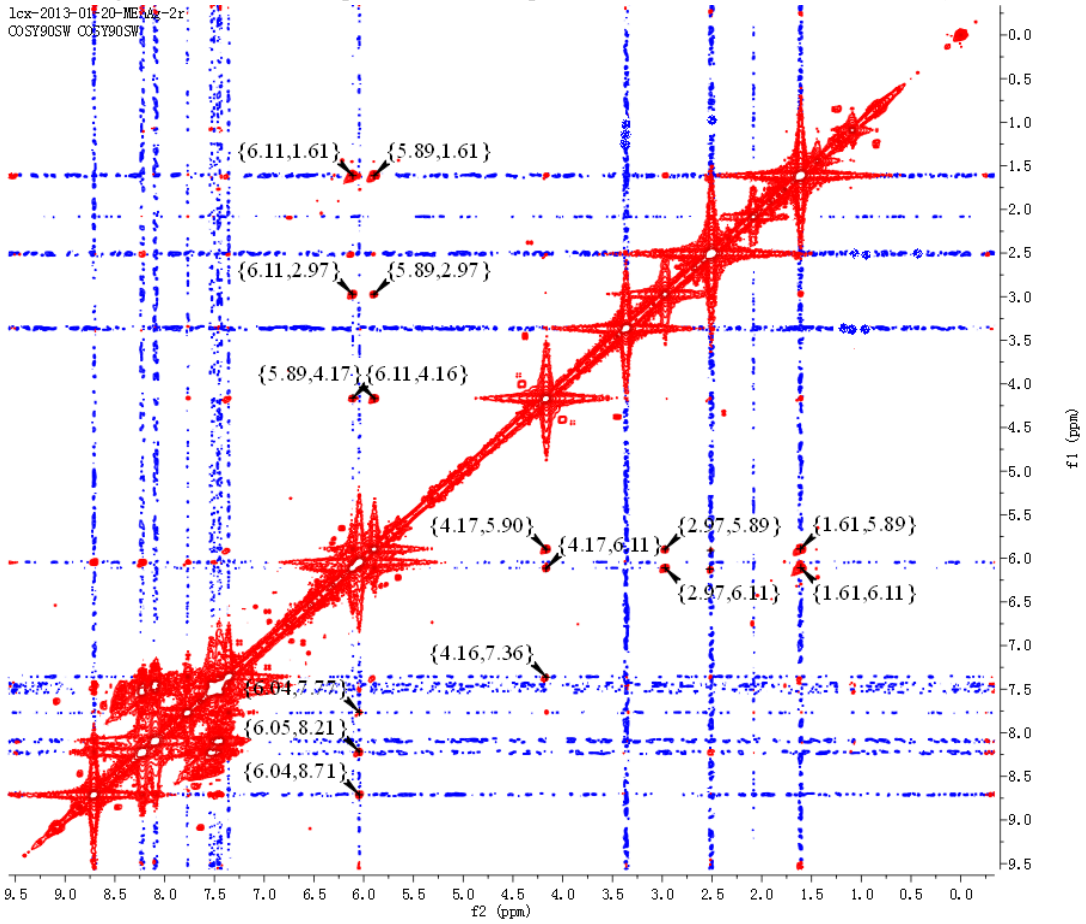

Figure S12. H-H COSY spectrum for complex **6e** (400 MHz, DMSO-d_6, 298 K)**.**

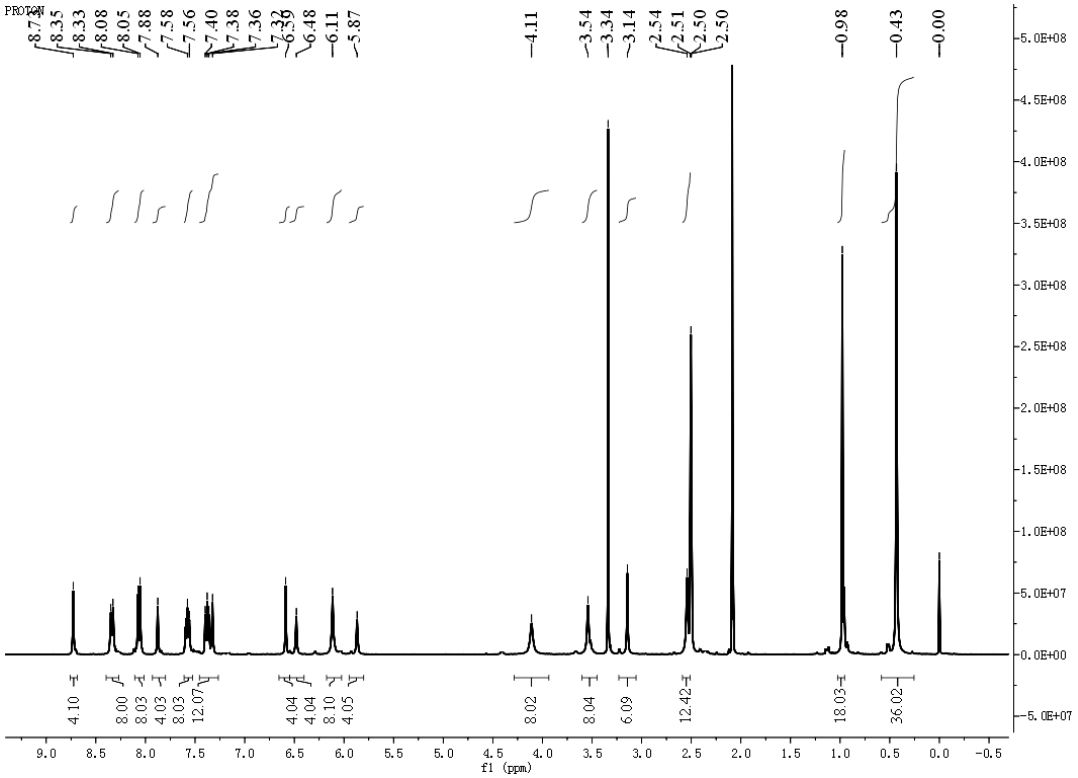

Figure S13. ^{1}H NMR spectrum for complex **6f** (400 MHz, DMSO-d_6, 298 K)**.**

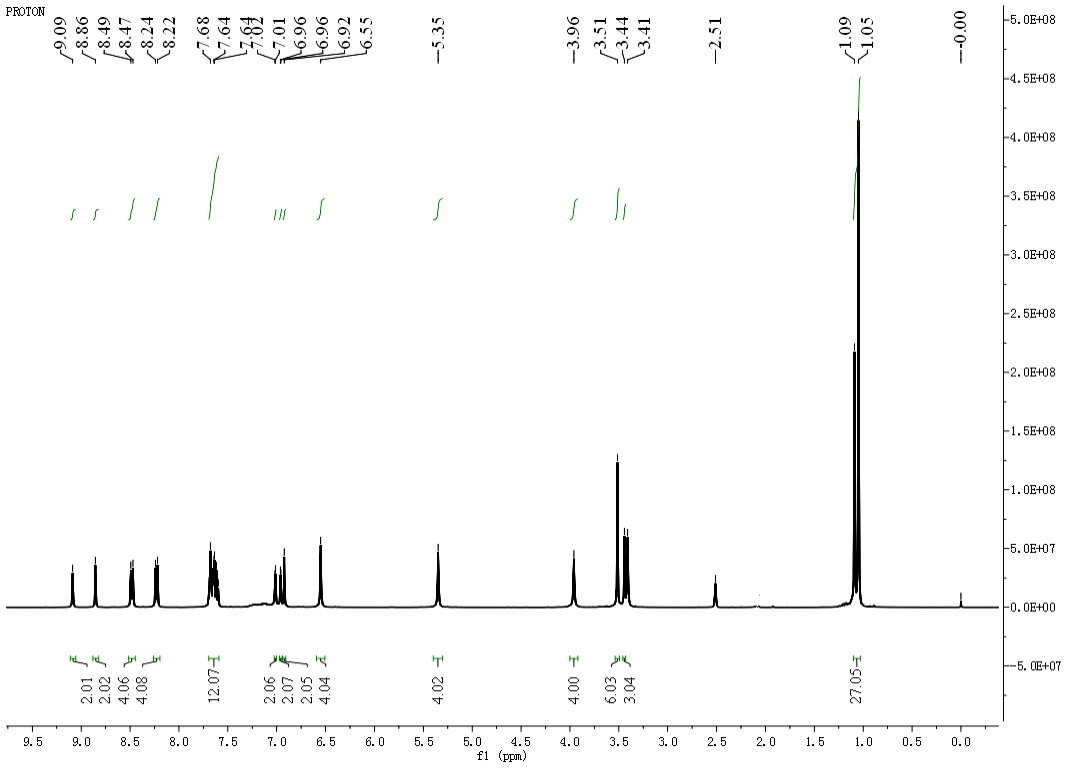

Figure S14. ^{1}H NMR spectrum for ligand **5f** (400 MHz, DMSO-d_6, 298 K)**.**

DOSY Experiment of complex 6d

DOSY experiment was performed at 298 K on a Bruker AV400 spectrometer equipped with an Accustar z-axis gradient amplifier and an ATMA BBO probe with a z-axis gradient coil. Maximum gradient strength was 0.214 T/m. The standard Bruker pulse program, dstebpgp1s, employing a double stimulated echo sequence, bipolar gradient pulses for diffusion, and one spoil gradient was utilized. Bipolar rectangular gradients were used with total durations 0.5-3 ms. Gradient recovery delays were 0.5-1 ms. Diffusion times were between 500 and 2000 ms. The quasi-2D diffusion databases were phased and baseline corrected.

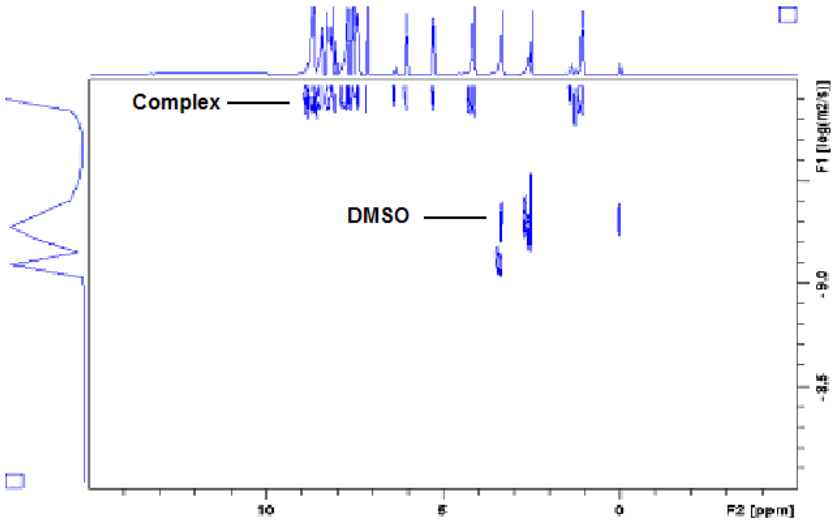

(a)

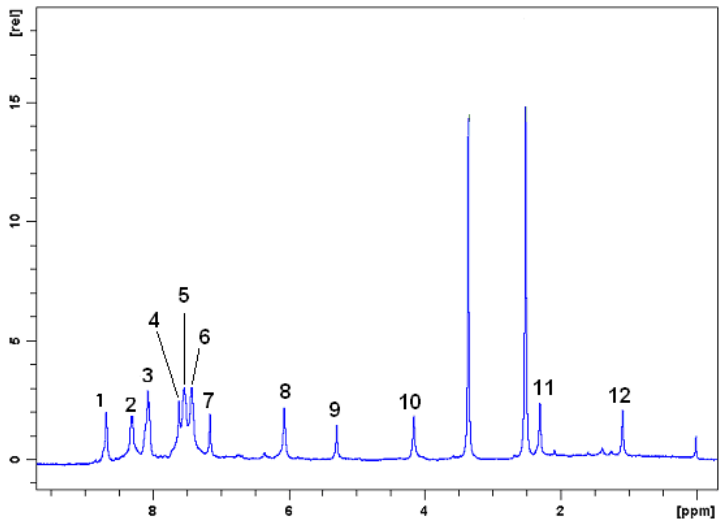

(b)

Figure S15. DOSY spectrum (a) and ^{1}H NMR spectrum (b) (400 MHz, DMSO, 25 °C) of the reaction mixture, which was obtained after treatment ligand **5d** with Ag_2O at 50 ^{o}C in acetonitrile overnight, filtered through the Celite to exclude the excess Ag_2O and removing the acetonitrile.

Table S3. The fitting diffusion coefficients (Diff Con.) corresponding to the DOSY spectrum in Figure S15.

Peak[a]	Peak Point (ppm)	Diff Con. (10^{-10} m^2/s)
1	8.672	1.020
2	8.311	1.008
3	8.065	1.016
4	7.605	1.037
5	7.530	1.032
6	7.417	1.018
7	7.149	1.006
8	6.060	1.016
9	5.287	1.011
10	4.152	1.015
11	2.298	1.028
12	1.086	1.018
		Average D = 1.019

[a] Some established characteristic ^{1}H NMR peak of complex **6d** in Figure S15b.

According to Stokes-Einstein equation: $D_{obs} = k_B T/6\pi\eta R_h$, where D_{obs} is the self-diffusion coefficients, k_B is the Boltzmann constant, T is the temperature and η is the viscosity of the solvent. The diffusion coefficients can give a rough size of the compound. The hydrodynamic radii (R_h) were calculated to be 10.78 Å.[1]

The strengths of the others peaks are less than 10%, and they did not give an identical diffusion coefficient. Others byproduct particles such as metal-ligand complexes of $[M_1L_1]$ or $[M_3L_3]$ type can not be detected from the DOSY-NMR experiments.

TGA, DSC and Variation temperature ^{1}H NMR of complex 6c

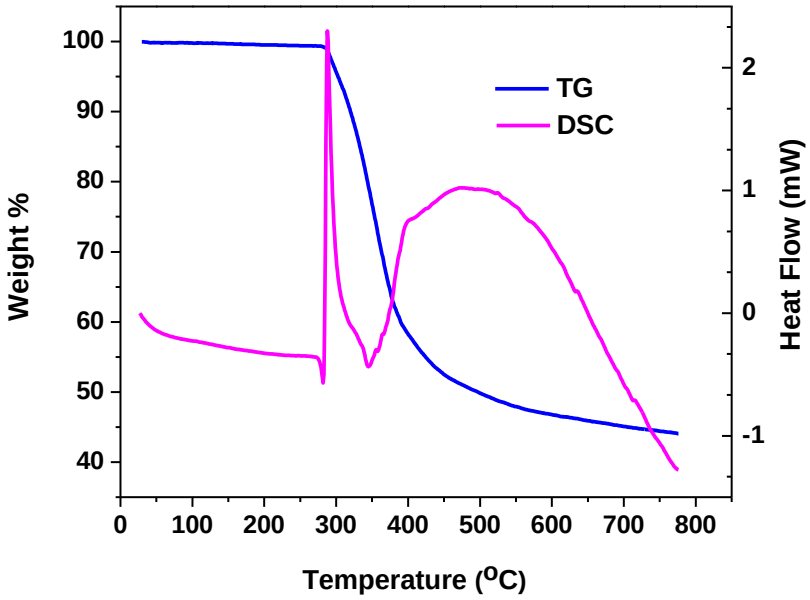

Figure S16. TGA and DSC curves of complex **6c**.

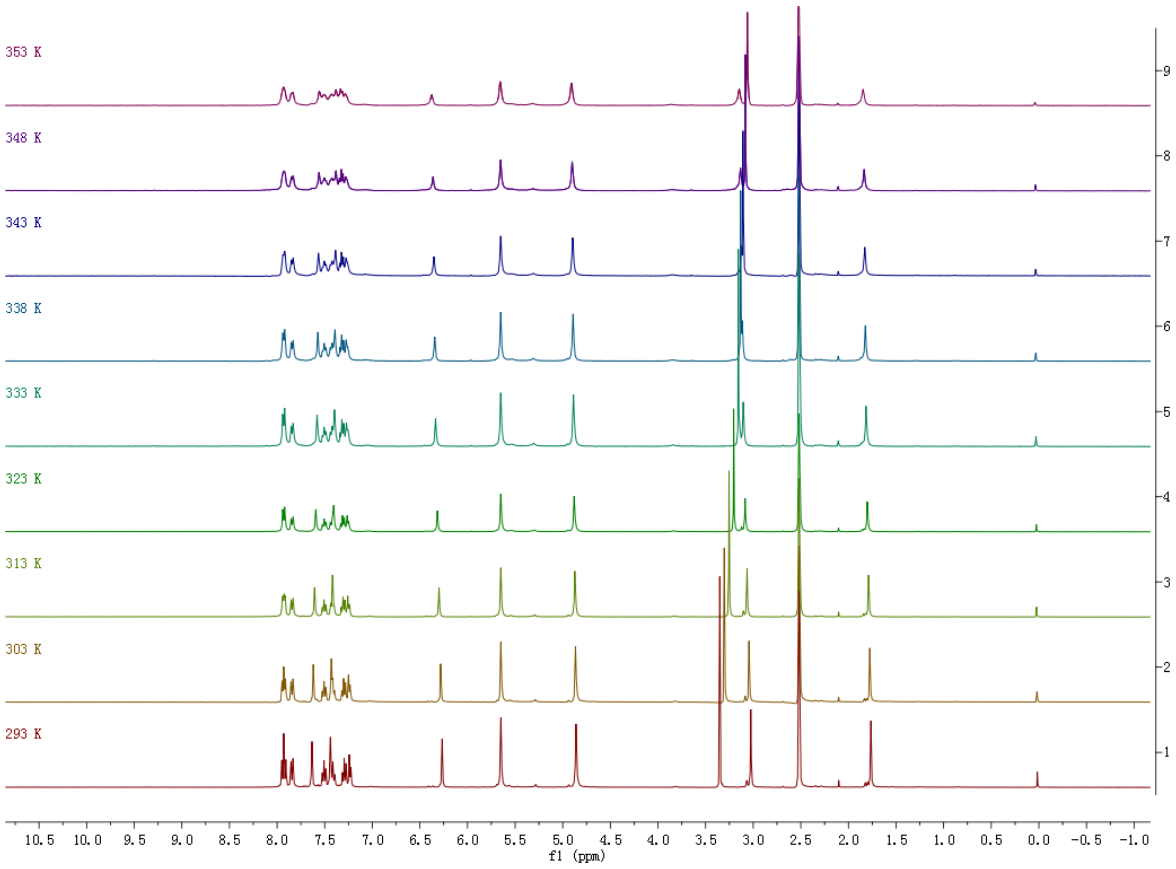

·Figure S17. Variation temperature ^{1}H NMR of complex **6c** (400 MHz, DMSO).

Stern-Volmer plot of 6d and BQ

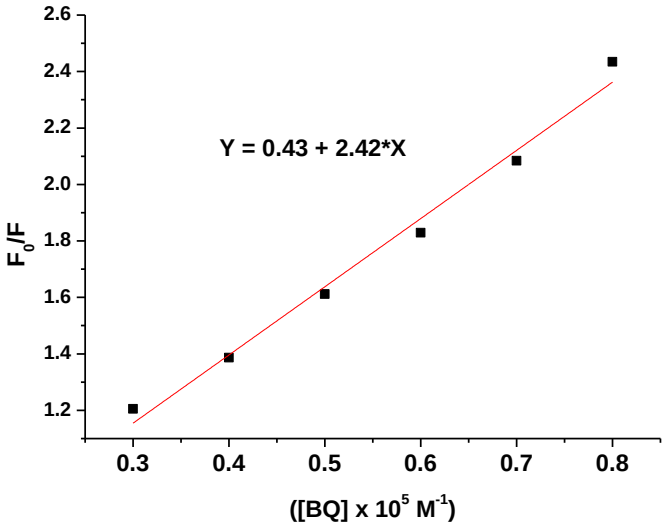

Figure S18. Stern-Volmer plot (λ_{ex} = 370 nm) of **6d** and **BQ** in acetonitrile. According to Stern-Volmer relation $F_0/F = 1 + K_a$ [Q], [Q] = the concentration of the quencher (guest). $K_a = 2.42\times10^5$ M^{-1}.

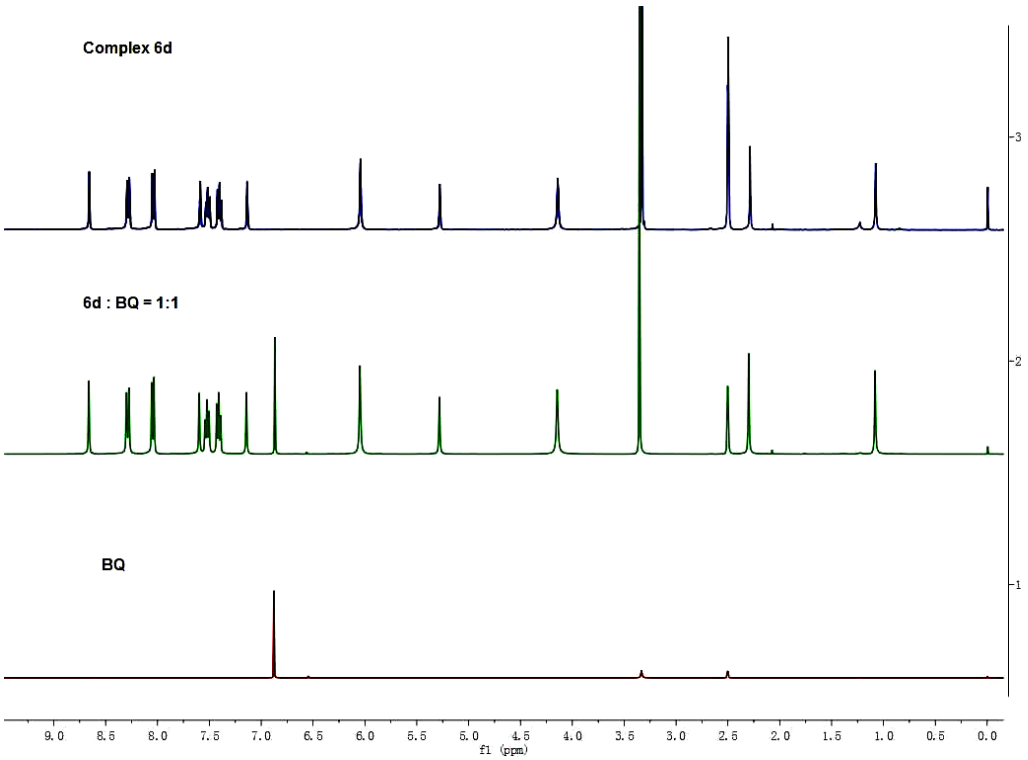

Figure S19. ^{1}H NMR spectrum of complex **6d** and **BQ** (400 MHz, DMSO-d_6, 298 K).

Job plot 1 of **6d/BQ** (done twice)

Table S4. Job plot 1 of **6d/BQ** [a]

x (mole fraction of **6d**)	F (emission intensity)	$x \cdot F_0$-F
1	448.90509 (F_0)	0
0.9	358.35602	45.65856
0.8	276.68112	82.44295
0.7	212.53974	101.69382
0.6	148.35145	120.9916
0.5	94.81054	129.642
0.4	58.31838	121.24366
0.3	30.13908	104.53245
0.2	16.43443	73.34659
0.1	10.80192	34.08859
0	1.11334	-1.11334

[a] Job plot of **6d** /**BQ** in acetonitrile solution at 416 nm.

Table S5. Job plot 2 of **6d/BQ** [a]

x (mole fraction of **6d**)	F (emission intensity)	$x \cdot F_0$-F
1	453.73489 (F_0)	0
0.9	353.42602	54.93538
0.8	274.51549	88.47242
0.7	214.99348	102.62094
0.6	148.4798	123.76113
0.5	95.16784	131.69961
0.4	57.94811	123.54585
0.3	28.44882	107.67165
0.2	18.96031	71.78667
0.1	13.46204	31.91145
0	3.17212	-3.17212

[a] Job plot of **6d** /**BQ** in acetonitrile solution at 416 nm.

Fluorescence titration of complex 6e with C_{60}

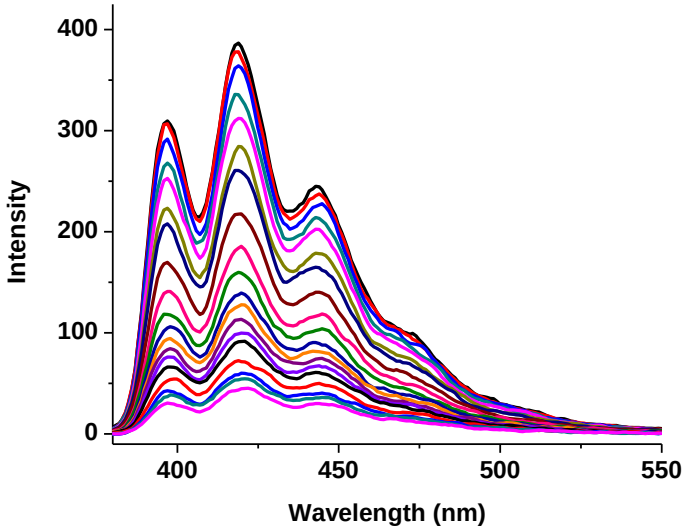

(a)

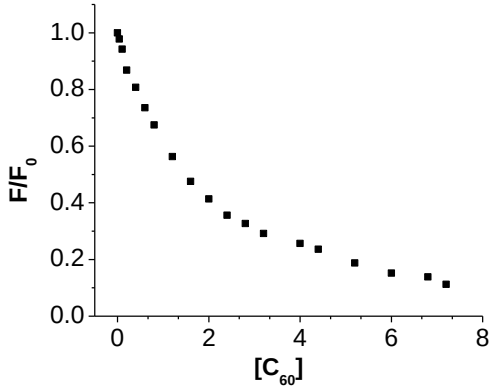

(b)

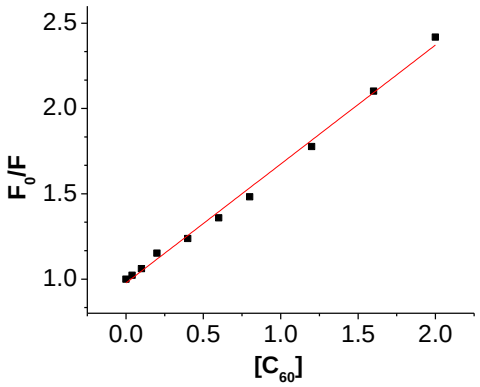

(c)

Figure S20 (a) Fluorescence spectra of complex **6e** (1.0×10^{-5} mol L^{-1}) with C_{60} in acetonitrile solution (λ_{ex} = 370 nm) at room temperature. The concentrations of C_{60} for curves from top to bottom are 0.0, 0.04, 0.1, 0.2, 0.4, 0.6, 0.8, 1.2, 1.6, 2.0, 2.4, 2.8, 3.2, 4.0, 4.4, 5.2, 6.0, 6.8, 7.2×10^{-5} mol L^{-1}. (b) Variation of fluorescence quenching F/F_0 of **6e** with increasing C_{60} concentration. (c) Stern-Volmer plot of receptor **6e** quenched by C_{60}.

$K_a = 6.97 \times 10^4\ M^{-1}$, $R^2 = 0.99457$.

Fluorescence titration of complex 6e with C_{70}

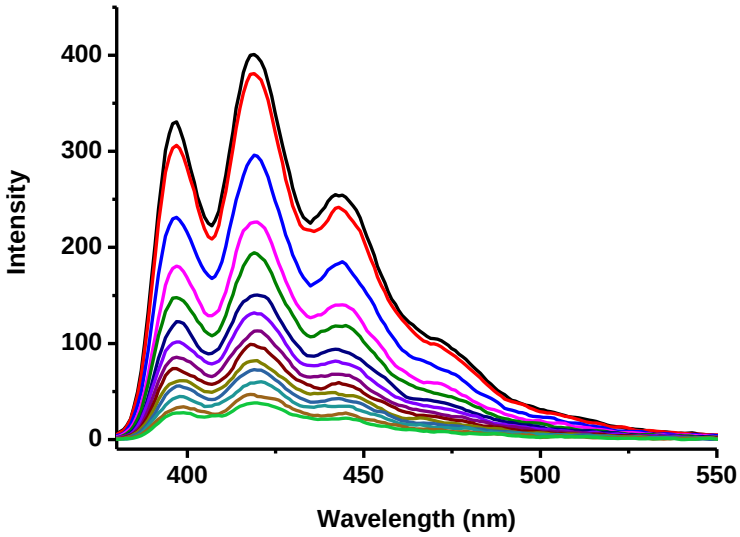

(a)

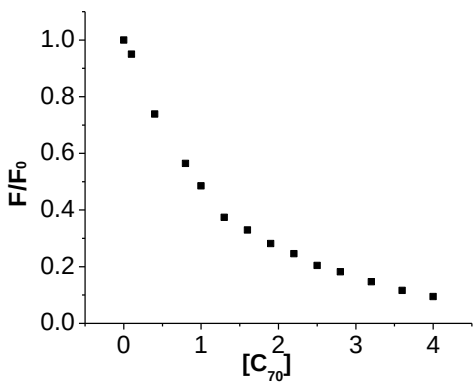

(b)

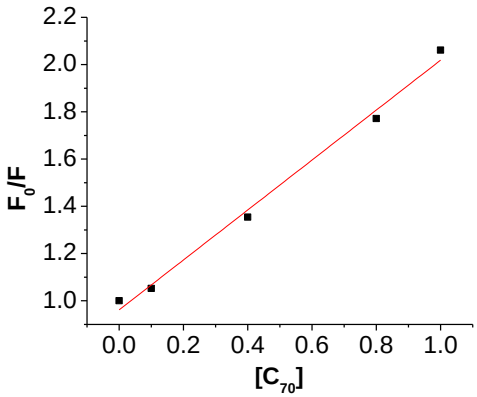

(c)

Figure S21 (a) Fluorescence spectra of complex **6e** (1.0×10^{-5} mol L^{-1}) with C_{70} in acetonitrile solution (λ_{ex} = 370 nm) at room temperature. The concentrations of C_{70} for curves from top to bottom are 0.0, 0.1, 0.4, 0.8, 1.0, 1.3, 1.6, 1.9, 2.2, 2.5, 2.8, 3.2, 3.6, 4.0×10^{-5} mol L^{-1}. (b) Variation of fluorescence quenching F/F_0 of **6e** with increasing C_{70} concentration. (c) Stern-Volmer plot of receptor **6e** quenched by C_{70}.

$K_a = 1.057 \times 10^5$ M^{-1}, $R^2 = 0.99107$.

Fluorescence titration of complex 6f with C_{60}

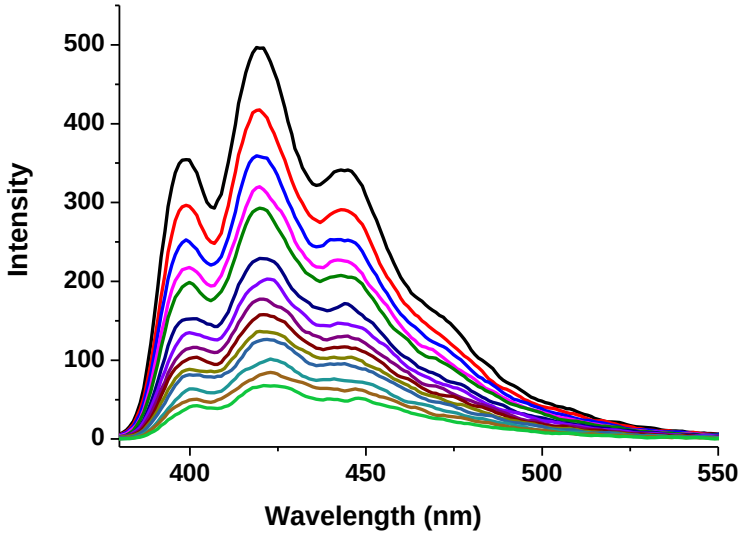

(a)

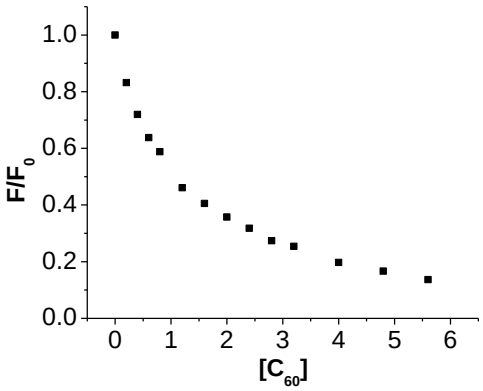

(b)

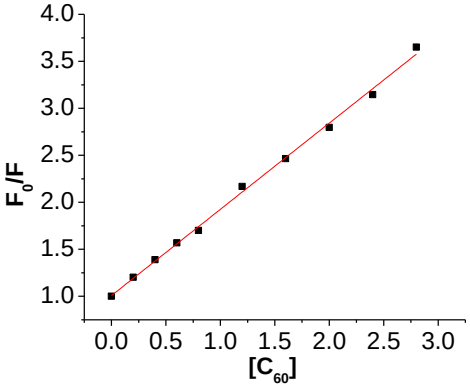

(c)

Figure S22 (a) Fluorescence spectra of complex **6f** (1.0×10^{-5} mol L^{-1}) with C_{60} in acetonitrile solution (λ_{ex} = 370 nm) at room temperature. The concentrations of C_{60} for curves from top to bottom are 0.0, 0.2, 0.4, 0.6, 0.8, 1.2, 1.6, 2.0, 2.4, 2.8, 3.2, 4.0, 4.8, 5.6×10^{-5} mol L^{-1}. (b) Variation of fluorescence quenching F/F_0 of **6f** with increasing C_{60} concentration. (c) Stern-Volmer plot of receptor **6f** quenched by C_{60}.

$K_a = 9.17 \times 10^4$ M^{-1}, $R^2 = 0.99722$.

Fluorescence titration of complex 6f with C_{70}

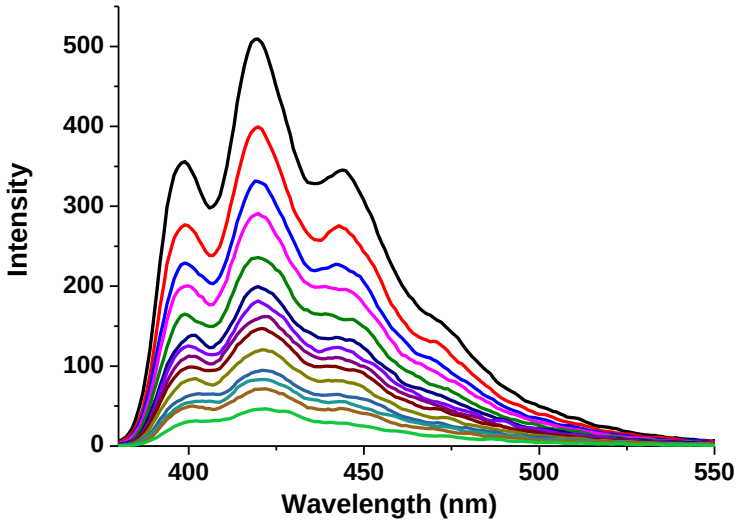

(a)

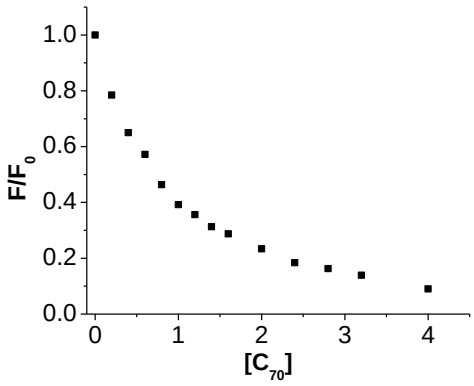

(b)

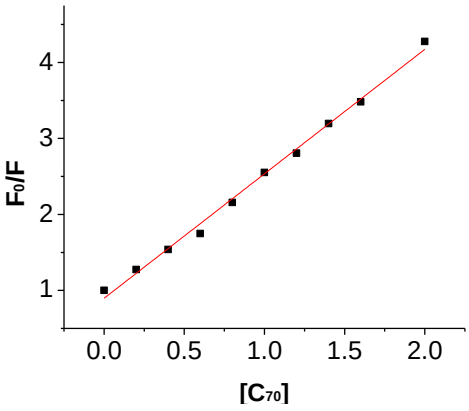

(c)

Figure S23 (a) Fluorescence spectra of complex **6f** (1.0×10^{-5} mol L^{-1}) with C_{70} in acetonitrile solution (λ_{ex} = 370 nm) at room temperature. The concentrations of C_{70} for curves from top to bottom are 0.0, 0.2, 0.4, 0.6, 0.8, 1.0, 1.2, 1.4, 1.6, 2.0, 2.4, 2.8, 3.2, 4.0×10^{-5} mol L^{-1}. (b) Variation of fluorescence quenching F/F_0 of **6f** with increasing C_{70} concentration. (c) Stern-Volmer plot of receptor **6f** quenched by C_{70}.

$K_a = 1.64 \times 10^5\ M^{-1}$, $R^2 = 0.99453$.

Reference

1. (a) R. S. Hickok, S. A. Wedge, A. L. Hansen, K. F. Morris, F. H. Billiot and I. M. Warner, *Magn. Reson. Chem.*, 2002, 40, 755-761; (b) R. Takano, K. Furumoto, K. Shiraki, N. Takata, Y. Hayashi, Y. Aso and S. Yamashita, *Pharmaceutical research*, 2008, 25, 2334-2344.